Intrinsic MSZW Characteristics of Racemic Species: Implication for Chiral Crystallization

Xiujuan Wang, Xia Yang, Yingxin Liu, and Chi Bun Ching
Div. of Chemical and Biomolecular Engineering, Nanyang Technological University of Singapore, 62 Nanyang Drive, Singapore 637459

DOI 10.1002/aic.11556
Published online July 10, 2008 in Wiley InterScience (www.interscience.wiley.com).

The metastable zone widths (MSZWs) of different racemic species in solutions were experimentally and theoretically investigated. It was found that the MSZWs of racemic conglomerates 4-hydroxy-2-pyrrolidone and N-methylephedrine were independent of enantiomeric excess, while the MSZWs of the racemic compound propranolol hydrochloride in different solvents were associated with the solubility ratio α of racemate to pure enantiomer. Crystal lattice properties were attributed to this difference. This can be used as the additional guideline for the characterization of racemic species. More interesting, abnormal apparent orders of primary nucleation rate at different enantiomeric excess were observed for conglomerate 4-hydroxy-2-pyrrolidone. It suggests a critical supersaturation exists beyond which the nucleation of the opposite isomer could occur. This phenomenon reveals particular implication of MSZW on the crucial supersaturation control during preferential crystallization, which was demonstrated in the preferential crystallization of 4-hydroxy-2-pyrrolidone with detailed modeling and in situ monitoring. © 2008 American Institute of Chemical Engineers *AIChE J,* 54: 2281–2292, 2008

Keywords: metastable zone width, nucleation, chiral, preferential crystallization, racemic species

Introduction

Because of the advantages of single enantiomers and the big chiral market, production of enantiomerically-pure materials using asymmetric methods, both in synthesis and separation, is very attractive. A racemic species can exist as a racemic conglomerate, a racemic compound or a pseudoracemate (Figure 1) based on its solid-state characteristic. Thermal analysis and structural studies by spectroscopy are normally used to identify the solid-state nature of racemic species.[1–4]

The application of preferential crystallization in the enantiomeric separation of pharmaceuticals and fine chemicals has become increasingly important from both practical as well as economic viewpoint.[5–9] Direct crystallization also shows big advantages for the enrichment of chiral compounds.[10–12] Most of the previous studies are focused on the chemistry aspects and the thermodynamic behaviors of solid phases.[1–4] Although metastable zone width (MSZW) is very useful in understanding the crystallization process in chiral resolution, not much attention has been paid on the measurement and interpretation of MSZW in the enantiomeric systems. Hongo et al.[13,14] identified the metastable region into two areas where the second one was more unstable. The dependence of MSZW on the enantiomeric excess was reported in the compounds of mandelic acid.[15,16] Our group recently started a series of characterization of MSZW of both conglomerate and racemic compound systems.[17–20] Furthermore, the metastable zone of the target enantiomer could be also closely related with the nucleation of the unwanted isomer.[8] Therefore, to measure and interpret the metastable zone of chiral system in solution should be very useful in understanding the chiral crystallization process, which has been rarely reported.

Correspondence concerning this article should be addressed to X. Wang at wangxj@ntu.edu.sg.

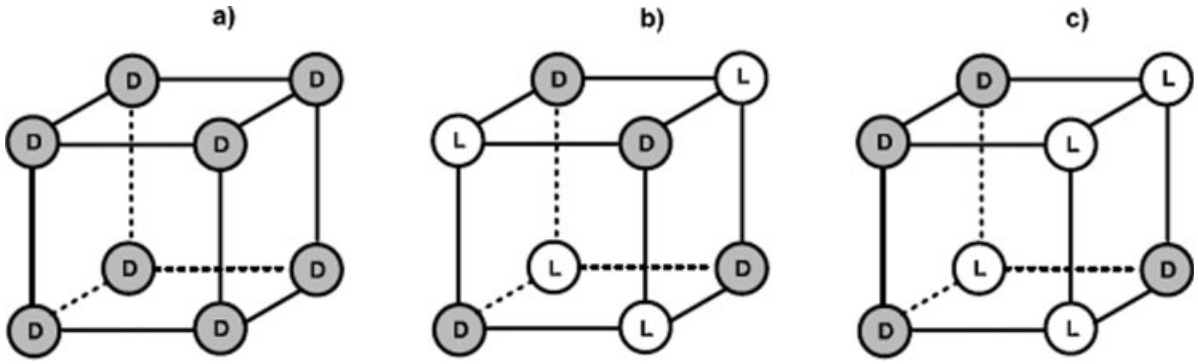

Figure 1. Crystal lattices of the three fundamental types of racemates.

(a) a conglomerate; (b) a racemic compound; (c) a pseudoracemate.

This work presents a detailed investigation of MSZW of different racemic species—conglomerates and racemic compound in solutions. The experimental data were analyzed with nucleation theory and crystal structural characteristics. The MSZW was found to be an inherent characteristic associated with thermodynamic properties of racemic species. For conglomerate, unusual unstable MSZW was identified and its particular implication in supersaturation control of preferential crystallization was illustrated.

Experimental

Materials

The (*R*)- and (*S*)-4-hydroxy-2-pyrrolidone, (+)- and (−)-*N*-methylephedrine, (*R*)- and (*S*)-propranolol hydrochloride were purchased from Sigma–Aldrich (Singapore) and were used as received. All enantiomers were stored in a refrigerator at about 5°C to reduce the risk of decomposition. The 4-hydroxy-2-pyrrolidone is a versatile chiral intermediate for the synthesis of many biological active compounds.[21] *N*-methylephedrine belongs to the class of ephedrines, which are potential central nervous stimulant drugs. Methylephedrine is an antitussive, which is contained in many over-the-counter cough and cold mediations, often mixed with other drugs.[22] Propranolol hydrochloride is a synthetic β-adrenergic receptor blocking agent widely used in the treatment of hypertension and cardiac arrhythmias.[23] Figure 2 shows the molecular structures of the above racemic species used in this work.

Analytical grade isopropanol and methanol were purchased from Aik Moh Paints & Chemicals (Singapore) and were used as received. The ultra pure deionized water was obtained through a Millipore ultrapure water system (Milli-Q Gradient A10 System).

Experimental set-up

The MSZWs of the solutions for racemate and its respective pure enantiomer were determined using a 35-ml jacketed glass crystallizer under same cooling conditions controlled by a Julabo FP 50-ME cooling circulator. Both visualization and a Lasentec S400A FBRM probe were used to detect the onset of nucleation and dissolution. MSZW depends on many variables; therefore all the experimental conditions were kept constant except for starting concentrations and cooling rate. Standard procedure was followed to carry out the MSZW measurements.[24] The values of solubility and MSZW were repeated three times to check the reproducibility. During the three repeated measurements, the deviation of MSZW was circa 0.6°C.

Cooling preferential crystallizations were carried out in a Mettler Toledo LabMax Automatic Laboratory Reactor system. As shown in Figure 3, it was equipped with a 600-ml jacketed curved-bottom glass crystallizer, a downward glass propeller stirrer driven by a heavy duty motor, a temperature sensor, a solenoid diaphragm dosing pump, and a balance. The temperature control and monitoring, solvent addition and stirring speed were performed in an automated and highly accurate mode. The temperature of the crystallizer was measured at 2-s intervals throughout a crystallization run. A Lasentec S400A FBRM was used for in situ monitoring the change of count number of the fine particles.

For a typical preferential crystallization, 20% ee *R*-enantiomer saturated solutions were prepared at circa 36°C. After slightly supersaturated at circa 35°C, pure *R*-enantiomer seeds were added into the solutions and cooled down from 35 to 5°C according to the proposed cooling profiles. The seeds were prepared by fast evaporating the solution of certain amount of pure *R*-enantiomer (circa 0.3 g) in isopropanol. The optical purity of crystal products were measured using a Mettler Toledo DSC 822^e Module (heat flux DSC), together with the STAR^e software. Samples of 3–6 mg were prepared in standard 40-μl aluminum crucibles. The crucibles were sealed with a perforated cover. The optical purity was also verified using a JASCO P-1020 digital polarimeter, which was equipped with a sodium vapor lamp emitting light with a wavelength of $\lambda = 589.3$ nm and a quartz cell of 50-mm path length. The crystal size distribution was measured using an off-line Malvern Mastersizer 2000 with a Hydro 2000 μP dispersion cell unit with *n*-hexane as the liquid dispersion medium.

Results and Discussion

MSZW of 4-hydroxy-2-pyrrolidone in isopropanol

The characterization and solubility of 4-hydroxy-2-pyrrolidone have been studied in our previous work and it was identified as a conglomerate.[19] The MSZWs of 4-hydroxy-2-pyrrolidone with different enantiomeric compositions (*R*-,

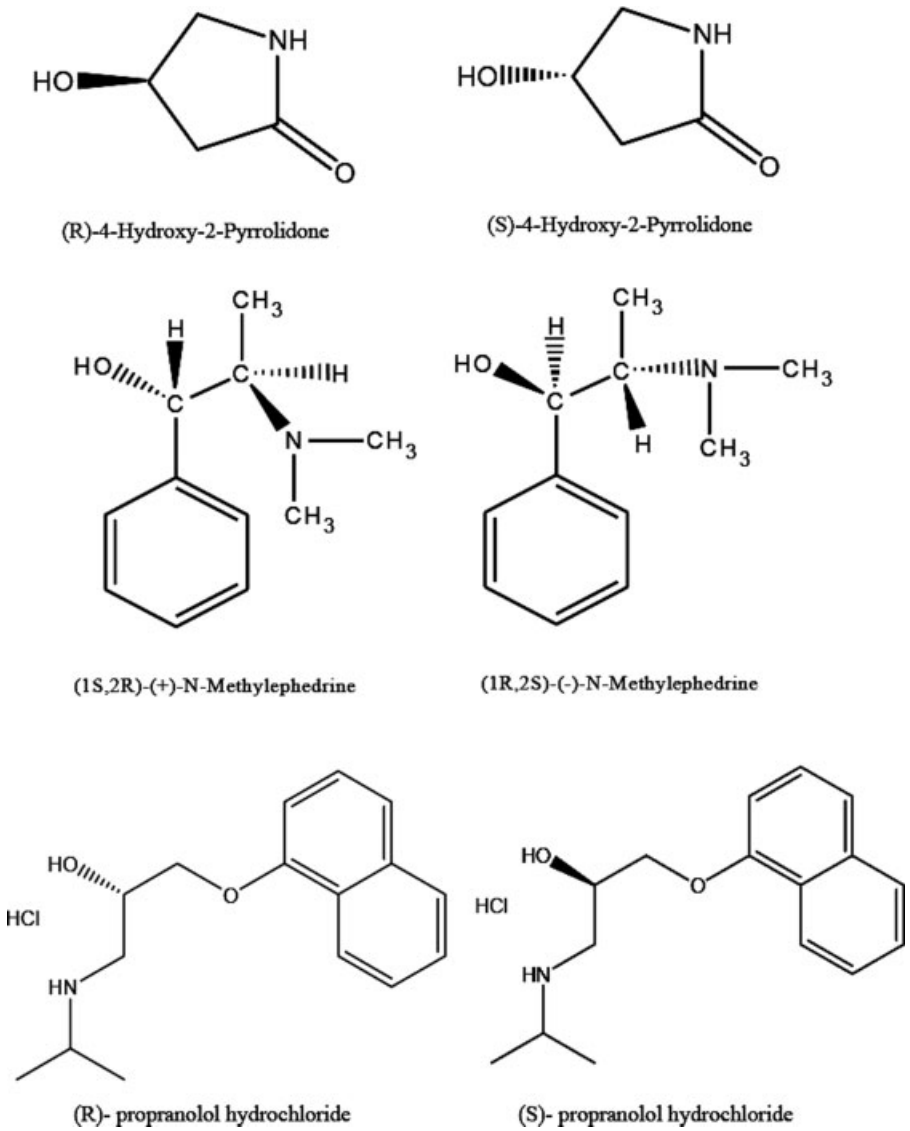

Figure 2. Molecular structures.

RS-, 20, 25, 40, 50, and 75% ee) under different cooling rates 1, 5, and 10°C/h are given in Figure 4. The MSZWs were determined using FBRM. The maximum allowable supersaturation was expressed in terms of the maximum allowable undercooling ($T_{\text{dissolution}} - T_{\text{nucleation}}$).

Figure 4 shows that the maximum allowable undercoolings greatly depend on the saturation temperatures as well as the cooling rates. When the cooling rate was constant, the MSZWs became narrower at higher saturation temperatures. This is consistent with the classical nucleation theory.[24] At higher temperature, the saturated solute concentration is higher. Therefore, there would be more molecules and more chances for molecule additions to reach the critical cluster which would result in faster nucleation and subsequent growth of the observable nucleus.

However, it is most interesting to notice that there was no significant difference of MSZWs under the similar operating conditions when the enantiomeric excess changed from 20 to 100% (pure *R*) although the corresponding solubility decreased almost 50%. This could be one of the characteristics of a conglomerate forming system. In solution, although the physical properties of both *R* and *S* are the same, the two enantiomers respond separately to form crystal nucleus, which means that the MSZW will be dependent on only concentration of isolated enantiomer. The following relationship of MSZWs with cooling rates will give some further quantitative analysis.

MSZW measurements are a simple method for estimation of relative nucleation data. Because of the lack of success of the classical nucleation theories in explaining the behavior of real systems, as discussed by Mullin,[24] the empirical power law is widely used to describe the primary nucleation in industrial crystallizer.

$$J = k_n \Delta c_{\max}^n \tag{1}$$

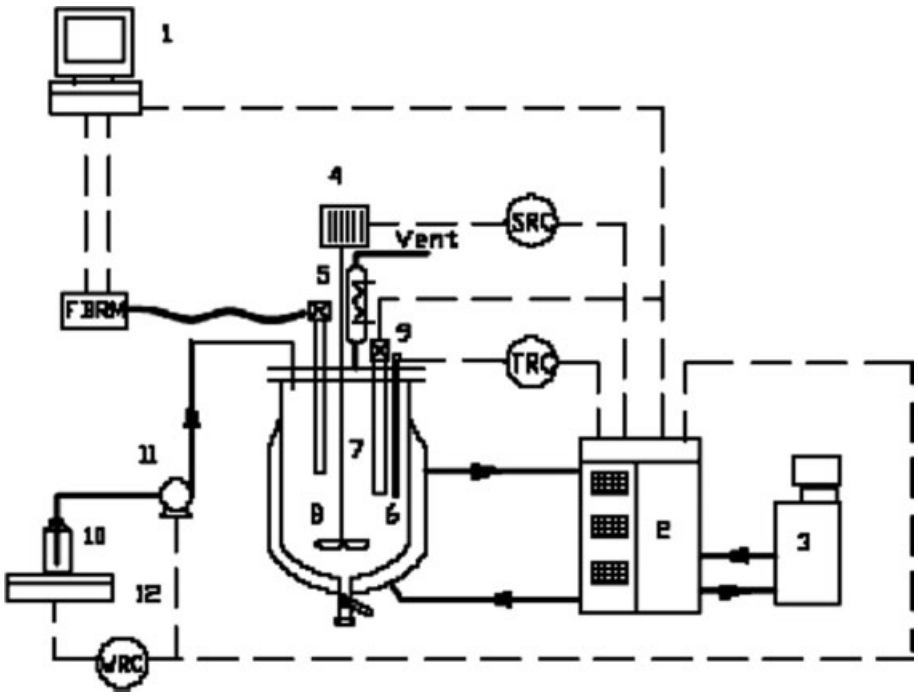

Figure 3. Experimental set-up.

(1) Computer; (2) LabMax; (3) Julabo cooling/heating refrigerator; (4) Heavy duty stirrer; (5) Condenser; (6) Temperature sensor; (7) 600-ml double-wall crystallizer; (8) FBRM; (9) PVM; (10) Solvent bottle; (11) Dosing pump; (12) Balance.

where J is the primary nucleation rate, k_n is the nucleation rate constant and Δc_{max} is the maximum allowable supersaturation (MSZW).

In the meantime, the nucleation rate can be derived from classical nucleation relationship by Nyvlt[25] in terms of cooling rate q.

$$J = q\frac{dC^*}{dT} \tag{2}$$

Assume that, at least in the initial stage of nucleation, the mass nucleation rate equals to the rate of production of supersaturation. The relationship of Δc_{max} and ΔT_{max} can be expressed as

$$\Delta c_{max} = \Delta T_{max}\frac{dC^*}{dT} \tag{3}$$

The above Eqs. 1–3 can be combined to get

$$\log q = n\log \Delta T_{max} + (n-1)\log\frac{dC^*}{dT} + \log k_n \tag{4}$$

This equation indicates that log q is linearly dependent on log ΔT_{max} with a straight line of slope n. This relationship is often used in laboratory to measure MSZWs.

Figure 5 presents the relationship of log ΔT_{max} with log q for *RS*, 20 and 25 ee% respectively. The regressed n and k_n are listed in Table 1. Good linearity can be observed for most of the data points. The nucleation rate constant k_n is normally dependent on temperature, but in the present system in the studied temperature range (5–40°C), this dependence is very small. Indeed, for RS, 20 and 25 ee% solutions, the k_n dependence on temperature is very weak. For higher ee solutions, large scatter of k_n is observed, especially for low concentration solutions. This could be due to the experimental error at low temperature measurements.

In Table 1, it is obvious that the apparent primary nucleation order (n = 5.3–7.4) of *RS* is generally smaller than those of other cases, especially pure *R* (n = 11–16). As we know, for conglomerate system, the two isomers respond separately to form crystal nucleus. Therefore, for solutions of pure *R* or with certain *R* enantiomeric excess, it is expected only *R* form nucleus at least during the very initial period and ΔT_{max} is only related with supersaturation of *R*. But for *RS*, two isomers should form nucleus at the same time and the contribution to the apparent nucleation rate is the addition of both *R* and *S* isomers. If the observable nucleation rate is assumed to be constant, Eq. 1 can be rewritten as

$$n = \frac{\log J/k_n}{\log \Delta c_{max}} \tag{5}$$

The nucleation rate constant k_n can be considered the same for both *R* and *S* enantiomers. Therefore, the above equation indicates the apparent primary nucleation order n for pure *R* or with certain ee% should be bigger than that of *RS* solution, which is what was exactly observed for most of data set in Table 1.

It is also very interesting to note that small apparent primary nucleation order n (circa 7–8) was also observed in several cases. This could be due to some extent of nucleation of *S*, which could initiate itself or could be induced by spontaneous nucleation of *R* when the supersaturation surpasses a critical level.

Actually, when high supersaturations within the metastable zone are used, some conglomerates will form crystals that

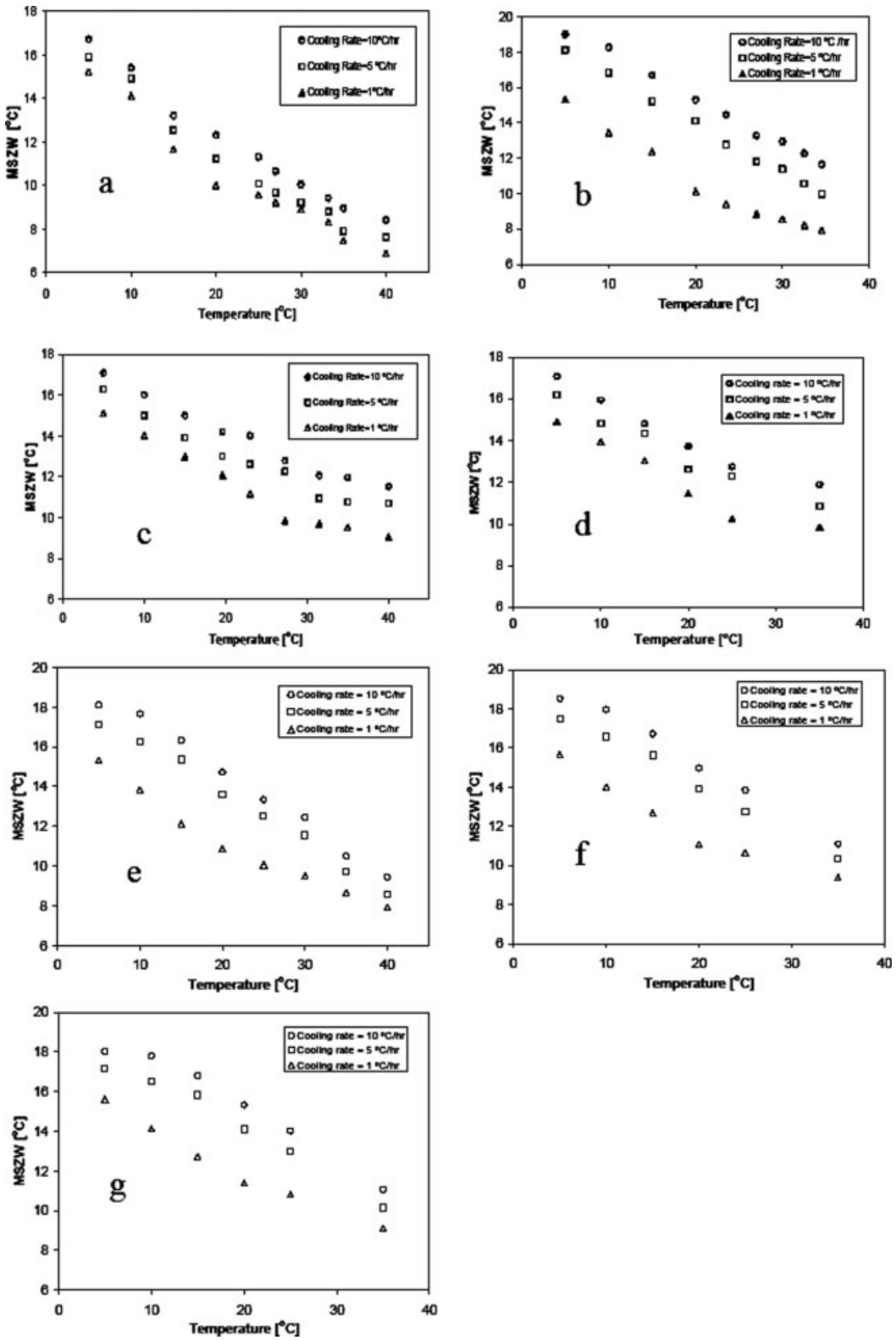

Figure 4. Experimental metastable zone widths of *R*-4-hydroxy-2-pyrrolidone in IPA for different cooling rates.

(a) R-, (b) RS-, (c) 20% ee, (d) 25% ee, (e) 40% ee, (f) %50 ee, and (g) 75% ee.

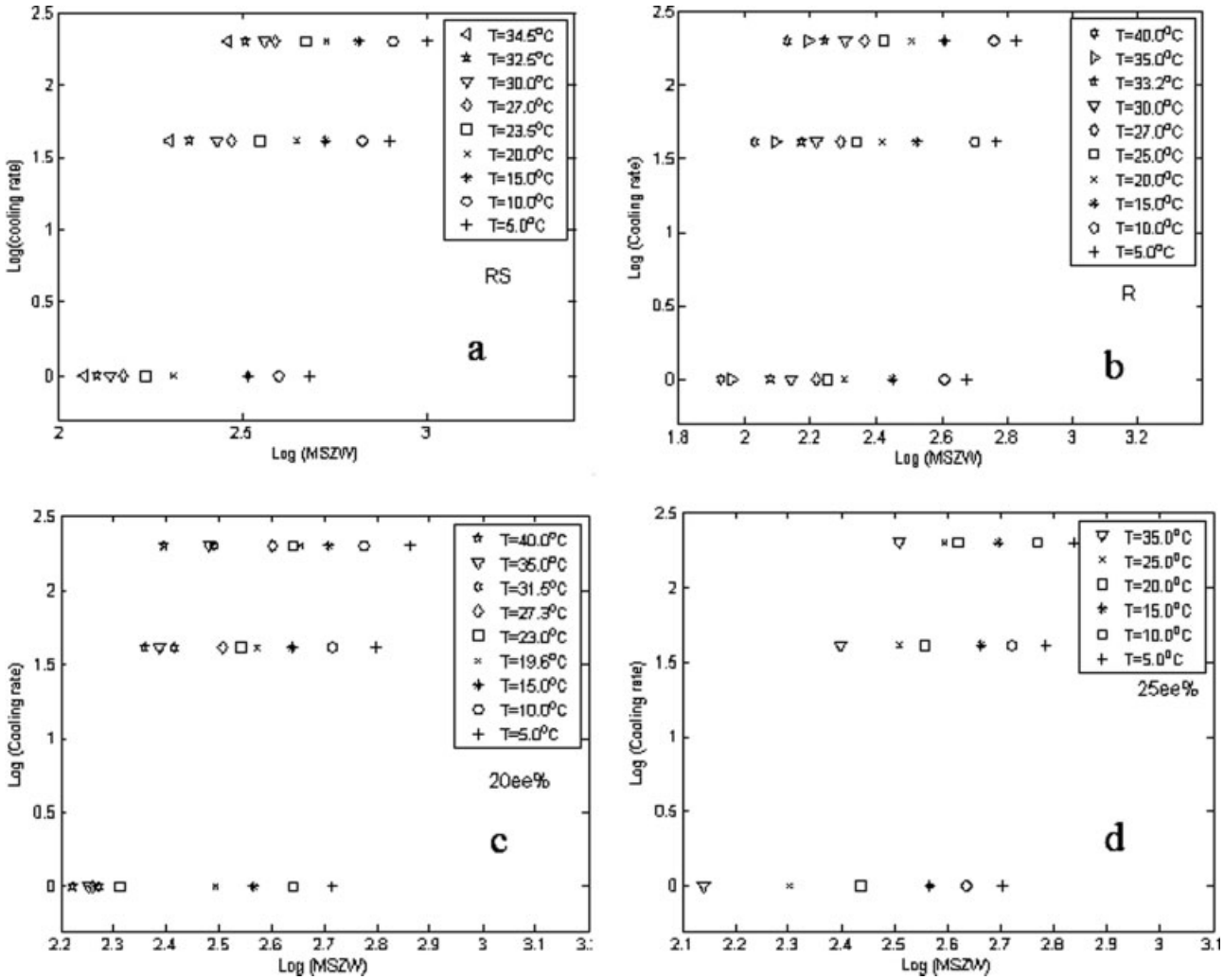

Figure 5. Relationship of log MSZW (log ΔT_{max}) with cooling rate (log q) for 4-hydroxy-2-pyrrolidone.

(a) RS, (b) R-, (c) 20% ee, and (d) 25% ee.

contain domains of both lattices in a single crystal, which means that the enantiomerically pure seed could nucleate the other enantiomer at its surface. One typical example is in the synthesis of agrochemical paclobutrazol where resolution of a racemic chiral ketone is involved.[26] Only when very low supersaturation (1°C undercooling) was used, did the effects of nucleating the unwanted isomer disappear to give the product with a high optical purity. This phenomenon at higher supersaturation was also observed on β-phenylglyceric acid.[27]

Hongo et al.[13,14] showed the stability of supersaturated DL-serine *m*-xylene-4-sulfonate dehydrate and identified two metastable regions where the supersaturation was relatively unstable in the second region. In the studies of nuclei breeding from a chiral crystal seed of $NaClO_3$,[28–30] it was found that at low supersaturation all nuclei were of the same chirality. At relatively high supercooling, but still lower than the critical value for spontaneous nucleation, many nuclei with opposite chirality to that of seed were formed. The similar findings were reported by Davey et al.[31] in triazolylketone chiral crystallization. The current experimental findings and those found in the literature, all of these suggest that even within the metastable zone, the supersaturation of target enantiomer is tightly associated with nucleation of its opposite enantiomer. This kind of nucleation is unwanted and should be inhibited in the preferential crystallization application.

MSZW of N-methylephedrine in the mixture of isopropanol and water

The characterization and solubility of *N*-methylephedrine have been studied in our previous work and it was also identified as a conglomerate.[18]

The MSZW measurements of *N*-methylephedrine in the mixture of isopropanol and water (Vol = 1:3) under cooling rate 2°C/h are given in Figure 6. When the cooling rate was constant, the MSZWs became narrower at higher saturation temperatures. Similar to that of 4-hydroxy-2-pyrrolidone system, the MSZW of *N*-methylephedrine in the mixture of isopropanol and water is also independent of enantiomer excess.

The MSZWs were measured at three cooling rates (2, 10, 30°C/h) and the relationship of log ΔT_{max} with log q is

Table 1. Regressed n and k_n for Different Concentrations of 4-Hydroxy-2-Pyrrolidone

ee%	T (°C)	n	k_n (m^{-3} s^{-1})
RS_4_HP	34.5	6.0	1.7×10^5
	32.5	5.8	1.4×10^5
	30.0	5.6	1.2×10^5
	27.0	5.6	1.6×10^5
	23.5	5.3	1.3×10^5
	20.0	5.3	1.8×10^5
	15.0	7.6	4.8×10^4
	10.0	7.4	8.0×10^4
	5.0	7.4	2.4×10^4
20% ee_R_4_HP	40.0	13.2	2.5×10^4
	35.0	10.4	2.3×10^4
	31.5	11.0	1.3×10^5
	27.3	7.1	1.6×10^5
	23.0	7.0	5.2×10^4
	19.6	14.3	3.0×10^5
	15.0	16.1	1.5×10^6
	10.0	16.8	2.2×10^5
	5.0	17.0	1.2×10^5
25% ee_R_4_HP	35.0	7.4	2.6×10^4
	25.0	8.4	8.5×10^4
	20.0	13.0	4.6×10^5
	15.0	17.8	1.7×10^5
	10.0	17.0	5.4×10^4
	5.0	17.1	1.7×10^5
40% ee_R_4_HP	40.0	13.2	1.9×10^5
	35.0	12.1	2.5×10^6
	30.0	8.5	1.5×10^5
	25.0	10.3	3.4×10^5
	20.0	8.4	2.8×10^6
	15.0	8.2	4.9×10^6
	10.0	11.4	1.5×10^7
	5.0	13.8	2.4×10^8
50% ee_R_4_HP	35.0	14.0	1.4×10^5
	25.0	8.8	2.0×10^5
	20.0	7.5	9.0×10^5
	15.0	8.2	2.3×10^6
	10.0	9.3	5.4×10^7
	5.0	14.0	3.2×10^8
75% ee_R_4_HP	35.0	12.0	1.3×10^7
	25.0	8.8	4.1×10^6
	20.0	7.7	4.6×10^6
	15.0	8.4	1.5×10^8
	10.0	10.4	1.6×10^9
	5.0	16.1	7.3×10^{10}
Pure R_4_HP	40.0	11.0	1.2×10^9
	35.0	12.3	1.9×10^9
	33.2	14.0	1.0×10^{10}
	30.0	14.1	1.1×10^{10}
	27.0	14.9	2.2×10^8
	25.0	12.4	4.3×10^8
	20.0	11.3	1.2×10^5
	15.0	14.2	5.9×10^8
	10.0	16.0	3.7×10^8
	5.0	14.8	2.3×10^{12}

shown in Figure 7. The regressed n for pure *N*-methylephedrine, 25 and 75 ee% is between 6.1 and 6.8, while n for racemic mixture is circa 4.3. This is again one of the characteristics for a conglomerate as observed in 4-hydroxy-2-pyrrolidone system.

MSZW of propranolol hydrochloride

The characterization of propranolol hydrochloride as a racemic compound system was reported in our previous study.[17] The solubility of propranolol hydrochloride in the mixture of methanol and isopropanol (Vol = 1:5) is shown in Table 2 and the solubility of propranolol hydrochloride in the mixture of water and isopropanol (Vol = 1:4) is shown in Table 3, where α is the solubility ratio of RS to R.

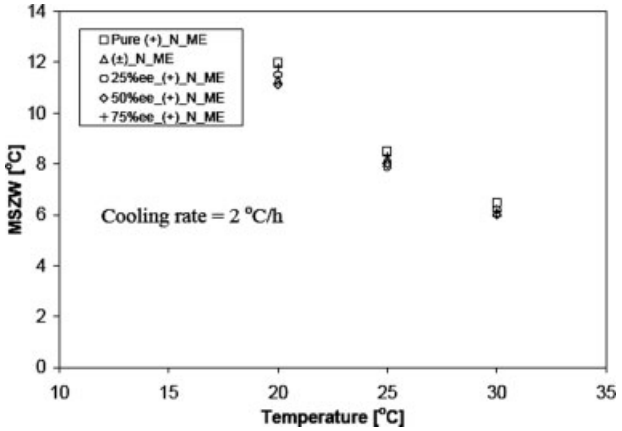

Figure 6. Experimental metastable zone widths of *N*-methylephedrine in the mixture of IPA and water (Vol = 1:3) for different enantiomeric excess.

The general trend of narrower MSZW with higher temperature is again observed here. However, unlike the conglomerates of 4-hydroxy-2-pyrrolidone and *N*-methylephedrine, which have similar MSZWs for the pure enantiomer and its corresponding racemic mixture, the MSZWs of pure (*R*)- and (*RS*)-propranolol hydrochloride are quite different. As shown in Table 2, under the same saturated temperature, (*RS*)- gave a wider MSZW than that of pure (*R*)-enantiomer, although the solubilities of RS were larger than R in the mixture of methanol and isopropanol (Vol = 1:5).

On the contrary, as shown in Table 3, under the same saturated temperature, (*RS*)- gave a smaller MSZW than that of pure (*R*)-enantiomer. The difference for the above two systems is in the solubility ratio α of RS to R in different solvents.

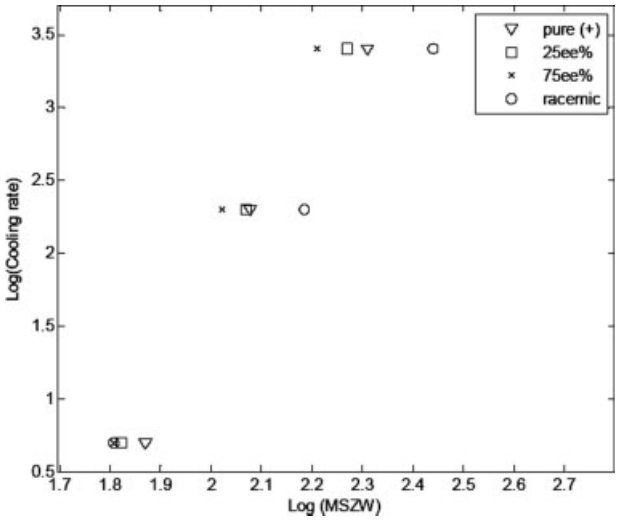

Figure 7. Relationship of log MSZW (log ΔT_{max}) with cooling rate (log q) for *N*-methylephedrine (T = 30.0°C).

Table 2. Solubilities and MSZWs of (*R*)- and (*RS*)-Propranolol Hydrochloride in the Mixture of Methanol and Isopropanol (Vol = 1:5)

T_{sat} (°C)	C_{RS} (mg Solute/ml Solvent)	C_R (mg Solute/ml Solvent)	α	ΔT_{max_RS} (°C)	δT_{max_R} (°C)
35.0	14.3	9.6	1.49	17.0	11.5
30.6	13.2	8.7	1.52	19.7	13.3
28.6	11.7	7.9	1.48	20.4	16.5
23.0	9.6	6.8	1.41	27.0	23.2
19.0	8.2	5.9	1.39	30.8	26.0
16.0	7.5	5.5	1.36	–	–
12.0	6.8	5.1	1.33	–	–

This interesting phenomenon could be explained from the arrangement of two enantiomer molecules in the crystal lattice for a racemic compound and classical nucleation theory.

As for a racemic compound, the two enantiomers form a 1-1 mixed well-defined crystal lattice in equal proportions (Figure 1b). According to the classical nucleation theory, the MSZW of *RS* will be dependent on the concentrations of both enantiomers. Since the solubility of *RS* is not definitely related to that of pure enantiomers and it can be either greater or smaller than that of pure-enantiomer,[1,2] three cases could arise.

(i) The solubility ratio α of racemate to pure enantiomer is smaller than 1 ($\alpha < 1$). In this case, the solubility of racemate is smaller than that of pure enantiomer. The MSZW of racemate is wider than that of pure enantiomer because less solute molecules are in the solution to undergo collision to form embryos and develop into nuclei. This case is widely observed in many racemic compound systems such as ketoprofen.[20]

(ii) The solubility of racemate is bigger than that of pure enantiomer, but the ratio is smaller than 2 ($1 < \alpha < 2$). In this case, although more molecules are in the solution, the *R*-molecules and *S*-molecules are required to arrange in equal quantities to form RS racemate. Therefore, the effective concentration to form nuclei is actually only half the total concentration. Since $\alpha < 2$, the effective *R* concentration (*R*:*S* = 0.5:0.5) is smaller than that of pure enantiomer. Therefore, the MSZW of racemate should be bigger than that of pure enantiomer. This is true for current studied racemic compound propranolol hydrochloride, where the solubility ratio of *RS* to *R* is bigger than 1 but less than 2 in the mixture of methanol and isopropanol (Vol = 1:5) as shown in Table 2. The similar phenomenon was also observed in the mandelic acid system.[15,16] The solubility of (DL)-mandelic acid is smaller than twice that of the (D)-mandelic acid approximately at certain temperature ranges of (0–25°C and 37–60°C). The corresponding MSZW of (DL)-mandelic acid is bigger than that of (D)-mandelic acid. This is unlike the above conglomerate systems where two enantiomers are not associated in solution and the MSZW is independent of enantiomeric excess.

(iii) The solubility of racemate is bigger than twice that of pure enantiomer ($\alpha > 2$). As mentioned above, the effective R concentration is bigger than that of pure enantiomer. In this case, the MSZW of racemate should be smaller than that of pure enantiomer. This is the case for propranolol hydrochloride in the mixture of water and isopropanol (Vol = 1:4) as shown in Table 3. This phenomenon was also observed in the mandelic acid system.[15,16] The solubilities of (DL)-mandelic acid are bigger than twice that of the (D)-mandelic acid approximately at certain temperature range of 23–36°C. The corresponding MSZW of (DL)-mandelic acid is smaller than that of (D)-mandelic acid.

The above analysis indicates a cut value of 2 of α is apparently related to the MSZW in racemic compound systems. This could be used as a new additional criterion to determine whether a racemate crystallizes as a racemic compound or conglomerate crystal. It could be particularly helpful when such a special racemic compound is met which shows quite similar other properties (for example, binary/ternary phase diagram of propranolol hydrochloride is similar to that of a conglomerate).[17,23]

Implications of MSZWs of 4-hydroxy-2-pyrrolidone in optical resolution by preferential crystallization

Preferential crystallization is an effective and cheap technology for optical resolution of conglomerates and it is normally operated as batchwise.[1–4] It consists of alternate selective nucleation/ crystallizations[32] of each antipode from a supersaturated mother liquor containing a slight excess of one enantiomer or even a supersaturated racemate solution, by seeding with respective pure enantiomer crystals.[1–3,5–9]

In view of thermodynamic aspects, it is crucial to keep the supersaturation of the undesired enantiomer in its metastable zone. But the present MSZW analysis suggests that it is paramount to control supersaturation within a critical value to avoid spontaneous nucleation of both enantiomers, to inhibit possible secondary initiated nucleation of undesired isomer

Table 3. Solubilities and MSZWs of (*R*)- and (*RS*)-Propranolol Hydrochloride in the Mixture of Water and Isopropanol (Vol = 1:4)

T_{sat} (°C)	C_{RS} (mg Solute/ml Solvent)	C_R (mg Solute/ml Solvent)	α	ΔT_{max_RS} (°C)	δT_{max_R} (°C)
40.0	74.5	13.4	5.6	15.1	22.9
35.0	53.4	11.1	4.8	16.2	25.3
30.0	33.0	7.5	4.4	17.9	27.9
25.0	24.6	7.2	3.4	19.2	>24.6
20.0	17.2	5.9	2.9	–	–

when the supersaturation surpasses a critical range. A saturated solution of 20 %ee *R*-4-hydroxy-2-pyrrolidone in isopropanol was used as the starting point to illustrate the importance of this kind of critical supersaturation control.

To control the supersaturation, a population balance is needed to model a batch crystallizer. Some general assumptions are made in order to simplify the mathematical model.

(i) The crystallization process proceeds in a batch crystallizer without input or output.

(ii) Crystal agglomeration and breakage are negligible.

(iii) The crystals in the crystallizer are well suspended without accumulation of crystals.

(iv) Crystal nuclei have negligible size.

With the above assumptions, the population balance is

$$\frac{\partial n(L,t)}{\partial t} + \frac{\partial [G(L,t)n(L,t)]}{\partial L} = 0 \tag{6}$$

where n is the population density of crystals and G is the crystal growth rate.

The orthogonal collocation method[33] was used here to solve the population balance equation to predict the cooling profile to control the supersaturation. The batch time period is divided into k time steps, each with length of Δt. At the time $t = j\,\Delta t$, $m + 1$ points are chosen to calculate the population density for the time $t = (j + 1)\Delta t$, with the size $L_{j,0}$, $L_{j,1}$, ..., $L_{j,m}$ and population densities $n_{j,0}$, $n_{j,1}$, ..., $n_{j,m}$. The first index ($j = 0,1,\ldots,k$) denotes the time interval number and the second index indicates the series number of points of the crystal size distribution.

For seed crystals,

$$\tilde{n}_{j+1,i} = \frac{\tilde{n}_{j,i}}{1 + \left.\frac{\partial G(L,t)}{\partial L}\right|_{L=L_{j,i},t=j\Delta t} \Delta t} \tag{7}$$

For newly formed crystals,

$$n_{j+1,i} = \frac{n_{j,i-1}}{1 + \left.\frac{\partial G(L,t)}{\partial L}\right|_{L=L_{j,i-1},t=j\Delta t} \Delta t} \tag{8}$$

Crystal size L can be expressed as

$$L_{j+1,i} \approx G(L_{j,i},j)\Delta t + L_{j,i} \tag{9}$$

The boundary condition is

$$n(L_0 = 0, t) = \frac{B^o}{G|L = 0} \tag{10}$$

Crystallization kinetics and solubility equation have been measured in our previous work.[8]

$$B = 3.4 \times 10^6 \times G^{1.9} \times M_T^{0.47} \tag{11}$$

$$G = 4.4 \times 10^5 \times \exp(-15000/RT) \times \Delta c^{1.35} \tag{12}$$

$$\Delta c(t) = c(t) - c^*(T(t)) \tag{13}$$

$$c^*(T) = 0.007227 + 0.000139(T - 273) + 8 \times 10^{-6}(T - 273)^2 \tag{14}$$

where B is the nucleation rate, M_T is the crystal suspension density and c^* is the solubility at temperature T.

The second moment of the distribution was used for mass balances, where h is a conversion factor equal to the volume of slurry per mass of solvent. Because the supersaturation is set as known, the energy balance is not required to project the cooling profile.

$$\frac{dc(t)}{dt} = -3\rho k_v h G m_2 \tag{15}$$

The above equations are combined together to obtain temperature profile for a given supersaturation Δc. For a saturated solution of 20% ee *R*-4-hydroxy-2-pyrrolidone in isopropanol, the starting temperature T_0 is circa 35°C. After seeding with *R*-enantiomer crystals, the solution can be cooled down until to circa 18°C where the solution tends to be racemic RS (0% ee). In this region, only *R*-enantiomer is supersaturated. Figure 4 indicates that the applicable supersaturation for *S*-enantiomer is 7–17°C. It should be noted that MSZW were measured in 35-ml crystallizer under homogenous condition and they should be narrower in the real world (larger size crystallizer and large crystals exist in the seeded preferential crystallization etc). More importantly, as present MSZW results suggest as well as suggested by Botsaris et al.,[13,14,28–31] at relatively high supercooling, but still lower than the critical value for spontaneous nucleation supercooling, many nuclei with opposite chirality to that of seed could form. Therefore, the supersaturation should be kept even low. As all these factors are taken into considerations, three supersaturations, namely Δc = 0.0018, 0.0020, and 0.0022 kg/kg solvent, were used to simulate the batch crystallization process. The calculated temperature via time curves are shown in Figure 8 respectively. They are typical cooling curves for batch crystallizer at constant supersaturation as the initial temperature decreases very slowly to prohibit unwanted nucleation while the temperature decreasing trend accelerates with time. Indeed, the simulated cooling profiles are also quite similar to those obtained from other simplified model.[8]

The temperature of the solutions inside the crystallizer was well controlled according to the proposed curves by the LabMax system. The chord length distributions over the whole crystallization process were recorded using FBRM as shown in Figure 9. A deep increase of fine counts (1–5 μm) was observed when Δc = 0.0022 kg/kg solvent was used, which implies that a sudden nucleation could happen at this time. There was no any evident change in the fine counts (1–5 μm) recorded for the other two cases.

The DSC thermograms of final crystal products obtained from the three experiments as well as the pure *R*-enantiomer and *RS* racemate are shown in Figure 10. The optical purity of the final crystal products were also verified by means of polarimetry. Table 4 lists the optical purities. When the supersaturation is Δc = 0.0018 and 0.0020 kg/kg solvent, the final crystals show very pure optical purity. This indicates that the induced nucleation of *S*-enantiomer was effectively inhibited by controlling the supersaturation of *R*-enantiomer within the current critical value (0.0020 kg/kg). This is also shown in the FBRM observations (Figure 9).

However, when the supersaturation exceeds this critical point, i.e., 0.0022 kg/kg solvent, the product optical purity begins to decrease to circa 85%. As discussed previously, this purity drop could come from the induced *S*-enantiomer

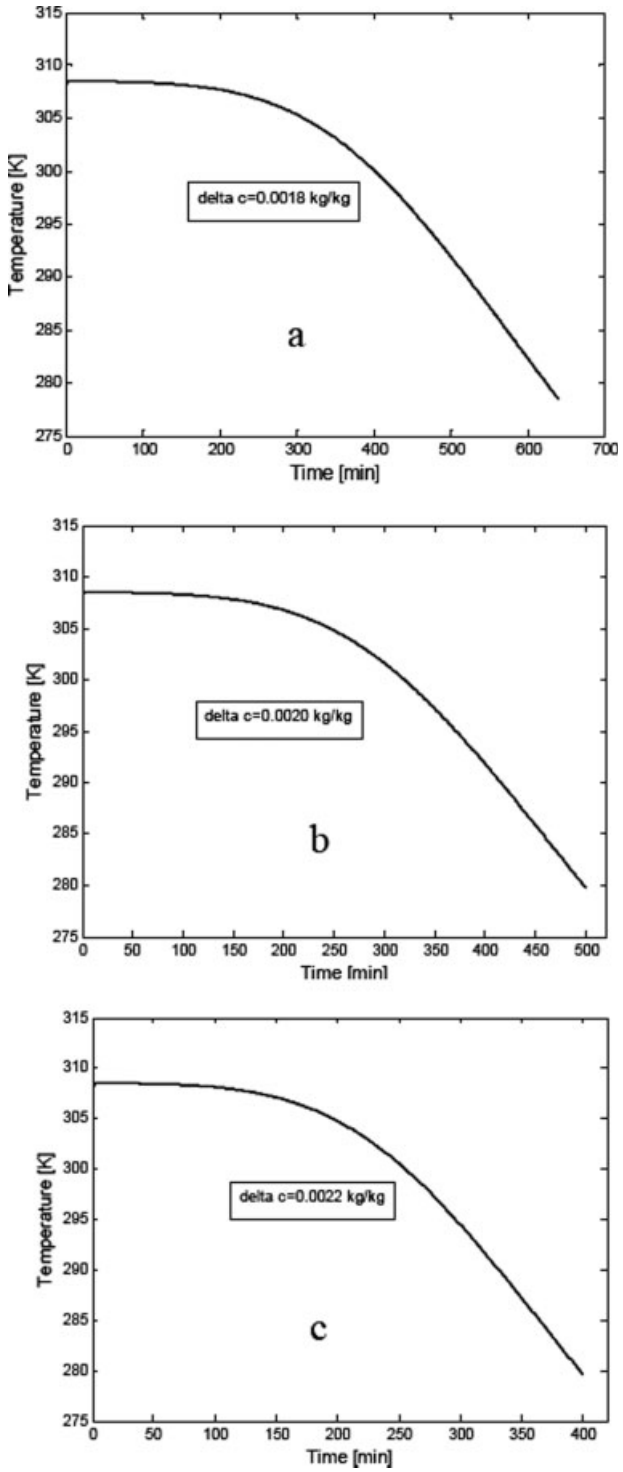

Figure 8. Cooling profile.

(a) $\Delta c = 0.0018$ kg/kg solvent, (b) $\Delta c = 0.0020$ kg/kg solvent, and (c) $\Delta c = 0.0022$ kg/kg solvent.

nucleation[13,26–31] when the supersaturation surpasses a certain level. Indeed, as shown in Figure 9c, a sudden nucleation was observed from the in situ chord length distribution using FBRM.

In the aspect of crystal size distribution and crystal habits, it is interesting to find that there is no significant difference for the three operations at different supersaturations. Figure 11a presents the crystal size distribution for the final crystal products. For comparison, the crystal size distribution of the prepared seeds as well as the simulated crystal size distribution of final crystals are also shown in Figure 11. It should be noted that the measured crystal size distribution does not perfectly match the simulated crystal size distribution, but the main shapes and the newly formed crystals are consistent with each other. This difficulty in recovering crystal size distribution from moment transformations has been well discussed by Rawlings et al.[34] Many efforts have been tried to optimize batch crystallization using various objectives, such as mean crystal size and coefficient of variation,[35,36] seed ratio,[37,38] and even shape.[39] But for preferential crystallization

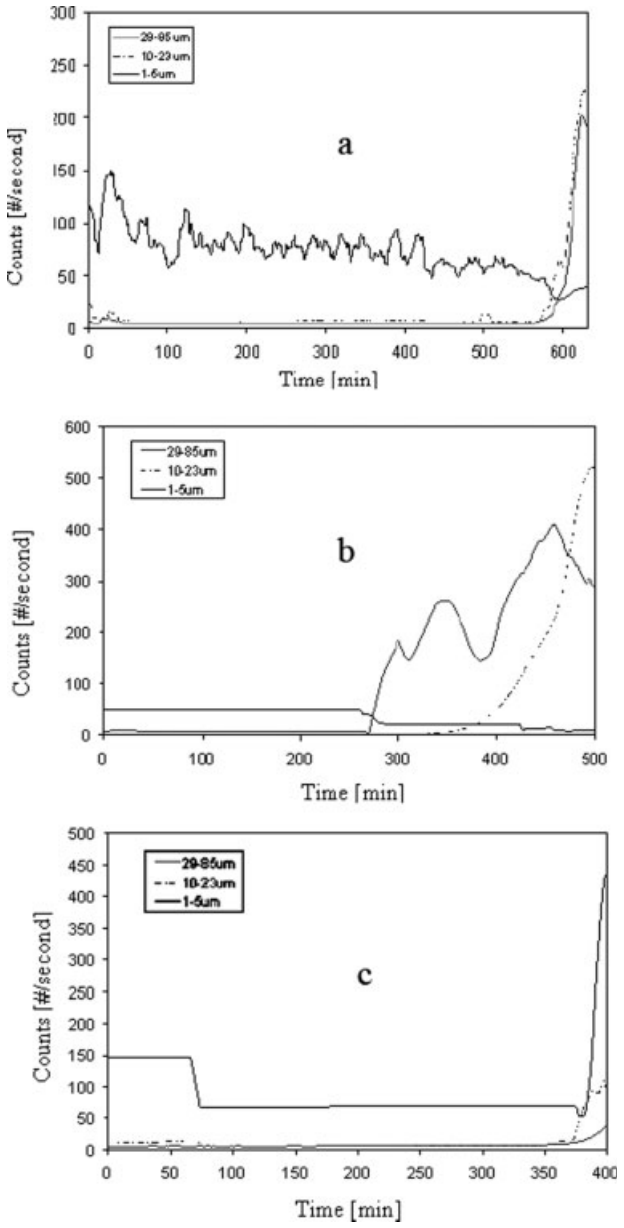

Figure 9. FBRM record of the number of fine counts.

(a) $\Delta c = 0.0018$ kg/kg solvent, (b) $\Delta c = 0.0020$ kg/kg solvent, and (c) $\Delta c = 0.0022$ kg/kg solvent.

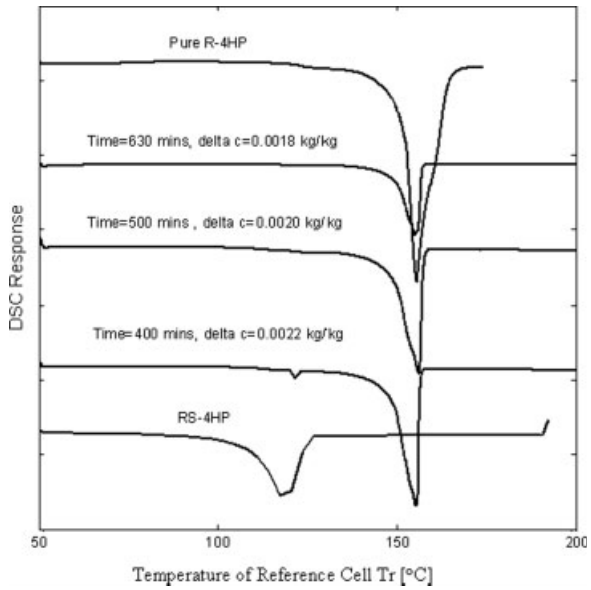

Figure 10. Product purities with different operating supersaturations.

process, current results show that the critical supersaturation is the most important factor to get high optical purity.

Conclusions

We investigated the characteristics and mechanism of MSZWs for two different racemic species- racemic conglomerate, and racemic compound. The MSZWs of both studied conglomerates 4-hydroxy-2-pyrrolidone and *N*-methylephedrine were found independent of enantiomer excess and the data at different cooling rates were in good agreement with classical nucleation theory. That is consistent with the characteristic of two enantiomers forming separate crystals for a racemic conglomerate. The different orders of primary nucleation rate at different enantiomeric excess indicate there may exist critical supersaturation beyond which the nucleation of opposite isomer could occur. This detailed experimental investigation of metastable zone in conglomerate system highlights crucial supersaturation control in preferential crystallization process.

For the racemic compound propranolol hydrochloride, its solubility characteristics and ternary phase diagram are quite similar to that of a conglomerate, but its MSZW was obviously dependent on the enantiomer excess. A cut value 2 of solubility ratio α was found to be correlated with the MSZW differences between racemate and pure enantiomers. The MSZWs of racemic compounds—mandelic acid and ketopro-

Table 4. Final Crystal Products Properties with Different Operating Supersaturations

Experiment	DSC Sample (mg)	Temperature (°C)	Polarimeter Sample (mg/10 g) IPA	α	Optical Purity (ee%)
δc = 0.0018 (kg/kg)	3.54	155	180	0.2602	100
Δc = 0.0020 (kg/kg)	3.31	155	180	0.2601	100
δc = 0.0022 (kg/kg)	5.24	153	180	0.2217	85.2

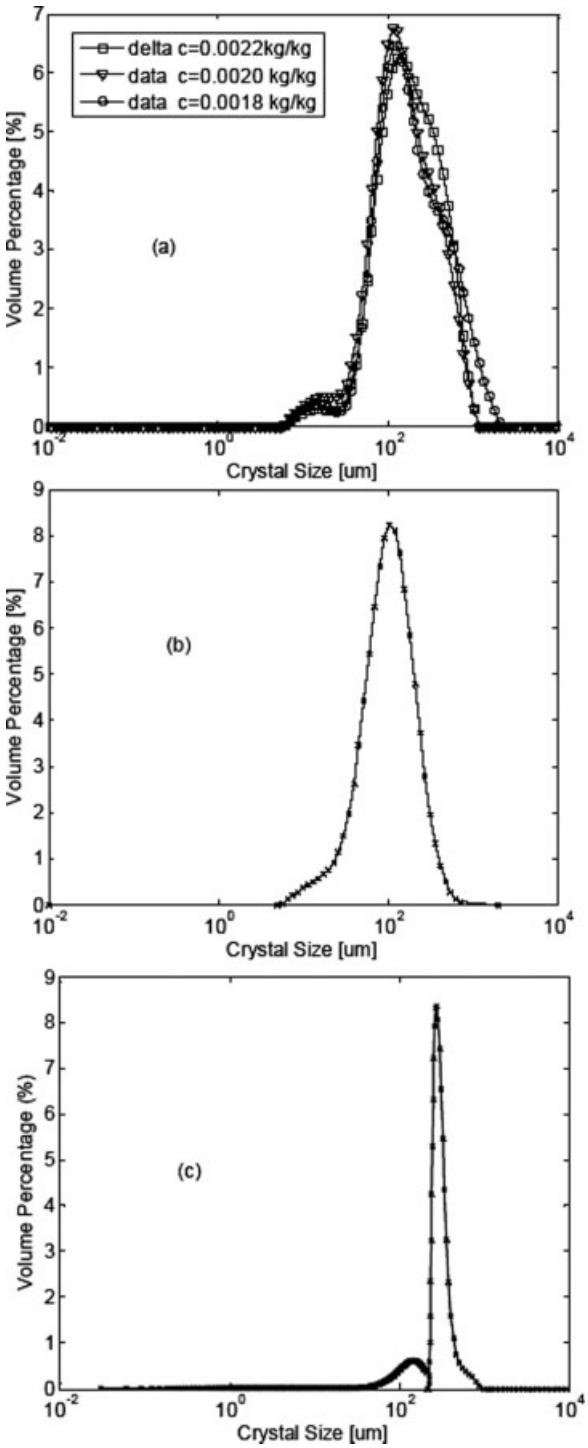

Figure 11. Crystal size distributions (a) from optimal operation at different supersaturations; (b) seed CSD; (c) Simulated final crystal size distribution; Δc = 0.0018 kg/kg solvent.

fen were also analysed and found to comply with the same findings. This reflects the properties of the evenly distributed molecules in the crystal lattice of a racemic compound. It suggests that MSZW can be used as an additional and important characteristic to identify these two kinds of racemates.

The implication of MSZW, particularly the existence of critical supersaturation in conglomerate system was demonstrated in the preferential crystallization of 4-hydroxy-2-pyrrolidone in isopropanol. The in situ monitoring shows that relatively high supersaturation of the target enantiomer induced spontaneous nucleation of the undesired enantiomer, which accordingly resulted in low optical purity. The proposed optimal temperature trajectory to control the critical supersaturation successfully inhibited the induced nucleation of the undesired enantiomer, and hence produced almost optically pure crystals.

Literature Cited

1. Collet AM, Brienne J, Jacques J. Optical resolution by direct crystallization of enantiomer mixtures. *Chem Rev*. 1980;80:215–230.
2. Jacques J, Collet A, Wilen SH. *Enantiomers, Racemates and Resolution*. Malabar, Florida: Krieger, 1994.
3. Li ZJ, Zell MT, Munson EJ, Grant JW. Characterization of racemic species of chiral drugs using thermal analysis, thermodynamic calculation, and structural studies. *J Pharm Sci*. 1999;88:337–346.
4. Coquerel G. Review on the heterogeneous equilibria between condensed phases in binary systems of enantiomers. *Enantiomer*. 2000;5:481–498.
5. Coquerel G. Preferential crystallization. *Top Curr Chem*. 2007; 269:1–51.
6. Schroer JW, Wibowo C, Ng KM. Synthesis of chiral crystallization processes. *AIChE J*. 2001;47:369–387.
7. Wood WML. Crystal science techniques in the manufacture of chiral compounds. In: Collins AN, Sheldrake GN, Crosby J, editors. *Chirality in Industry II*. Chichester: Wiley, 1997:119–155.
8. Wang XJ, Ching CB. A systematic approach for preferential crystallization of 4-hydroxy-2-pyrrolidone: thermodynamics, kinetics, optimal operation and in-situ monitoring aspects. *Chem Eng Sci*. 2006;61:2406–2417.
9. Beilles S, Cardinael P, Ndzie E, Petit S, Coquerel G. Preferential crystallization and comparative crystal growth study between pure enantiomer and racemic mixture of a chiral molecule: 5-ethyl-5-methylhydantoin. *Chem Eng Sci*. 2001;56:2281–2294.
10. Lorenz H, Sheehan P, Seidel-Morgenstern A. Coupling of simulated moving bed chromatography and fractional crystallisation for efficient enantioseparation. *J Chromatogr A*. 2001;908:201–214.
11. Fung KY, Ng KM, Wibowo C. Experimental study of the effect of buffer on chromatography and crystallization hybrid process. *Ind Eng Chem Res*. 2006;45:8393–8399.
12. Wang XJ, Lu J, Ching CB. Application of direct crystallization for racemic compound propranolol hydrochloride. *J Pharm Sci*. 2007; 96:2735–2745.
13. Hongo C, Yamada S, Chibata I. The prediction of the optical resolution process by the use of the preferential crystallization procedure. *Bull Chem Soc Jpn*. 1981;54:1911–1913.
14. Hongo C, Yamada S, Chibata I. The stability of supersaturation state in optical resolution by the preferential crystallization procedure. *Bull Chem Soc Jpn*. 1981;54:1905–1910.
15. Perlberg A, Lorenz H, Seidel-Morgenstern A. Determination of crystallization relevant data for enantioseparation purposes. In: Chianese A, editor. *Proceedings of 15th International Symposium on Industrial Crystallization*. Sorento, Italy. 2002:173–178.
16. Perlberg A, Lorenz H, Seidel-Morgenstern A. Determination of crystallization kinetics in chiral systems. In: Coquerel G, editor. *Proceedings of 10th International Workshop on Industrial Crystallization (BIWIC)*. Rouen, France. 2003:180–187.
17. Wang X, Wang XJ, Ching CB. Solubility, metastable zone width, and racemic characterization of propranolol hydrochloride. *Chirality*. 2002;14:318–324.
18. Wang XJ, Wiehler H, Ching CB. Physicochemical properties and the crystallization thermodynamics of the pure enantiomer and the racemate for *N*-methylephedrine. *J Chem Eng Data*. 2003;48:1092–1098.
19. Wang XJ, Wiehler H, Ching CB. Study of the characterization and crystallization of 4-hydroxy-2-pyrrolidone. *Chirality*. 2004;16:220–227.
20. Lu YH, Ching CB. Study on the metastable zone width of ketoprofen. *Chirality*. 2006;18:239–244.
21. Aube J, Wang Y, Ghosh S, Lnghans KL. Oxaziridine-mediated ring expansions of substituted cyclobutanones: synthesis of (−)-γ-amino-β-hydroxybutyric acid (GABOB). *Synth Commun*. 1991;21: 693–701.
22. Herraez-Hernandez R, Campins-Falco P. Chiral separation of ephedrines by liquid chromatography using β-cyclodextrines. *Anal Chim Acta*. 2001;434:315–324.
23. Neau SH, Shinwari MK, Hellmuth EW. Melting point phase diagrams of free base and hydrochloride salts of bevantolol, pindolol and propranolol. *Int J Pharm*. 1993;99:303–310.
24. Mullin JW. *Crystallization*. Oxford: Butterworth-Heinemann, 2001.
25. Nyvlt J. Kinetics of nucleation in solutions. *J Cryst Growth*. 1968;3/4:377–383.
26. Black SN, Williams LJ, Davey RJ, Moffatt F, Jones RVH, McEwan DM, Sadler DE. The preparation of enantiomers of paclobutrazol: a crystal chemistry approach. *Tetrahedron*. 1989;45:2677–2682.
27. Furberg S, Hassel O. Phenylglyceric acids. *Acta Chem Scand*. 1950;4:1020–1023.
28. Qian RY, Botsaris GD. Nuclei breeding from a chiral crystal seed of $NaClO_3$. *Chem Eng Sci*. 1998;53:1745–1756.
29. Kondepudi DK, Kaufman RJ, Singh N. Chiral symmetry breaking in sodium chlorate crystallization. *Science*. 1990;250:975–977.
30. McBride JM, Carter RL. Spontaneous resolution by stirred crystallization. *Angew Chem Int Ed Engl*. 1991;30:293–295.
31. Davey RJ, Black SN, Williams LJ, McEwan DM, Sadler DE. The chiral purity of a triazolylketone crystallized from racemic solutions. *J Cryst Growth*. 1990;102:97–102.
32. O'Dell FP, Rousseau RW, McCabe WL. Selective nucleation of mutually soluble substances. *Inst Chem Eng Symp Ser*. 1978;54:13–20.
33. Hu Q, Rohani S, Wang DX, Jutan A. Nonlinear kinetic parameter estimation for batch cooling seeded crystallization. *AIChE J*. 2004;50:1786–1794.
34. Rawlings JB, Miller SM, Witkowskit WR. Model identification and control of solution crystallization processes: a review. *Ind Eng Chem Res*. 1993;32:1275–1296.
35. Choong KL, Smith R. Optimization of batch cooling crystallization. *Chem Eng Sci*. 2004;59:313–327.
36. Costa CBB, Maciel Filho R. Evaluation of optimisation techniques and control variable formulations for a batch cooling crystallization process. *Chem Eng Sci*. 2005;60:5312–5322.
37. Matthews HB, Rawlings JB. Batch crystallization of a photochemical: modeling, control, and filtration. *AIChE J*. 1998;44:1119–1127.
38. Chung SH, Ma DL, Braatz RD. Optimal seeding in batch crystallization. *Can J Chem Eng*. 1999;77:590–596.
39. Ma DL, Braatz RD. Optimal control and simulation of multidimensional crystallization processes. *Comput Chem Eng*. 2002;26:1103–1116.

Manuscript received July 14, 2007, revision received Mar. 13, 2008, and final revision received May 14, 2008